Numer. Math. Theor. Meth. Appl.
doi: 10.4208/nmtma.2014.1305si

Vol. **7**, No. 4, pp. 435-446
November 2014

A Robin-Robin Domain Decomposition Method for a Stokes-Darcy Structure Interaction with a Locally Modified Mesh

Zhaohui Wang, Zhilin Li and Sharon Lubkin*

Department of Mathematics and Center for Research in Scientific Computation (CRSC), North Carolina State University, Raleigh, NC 27695, USA.

Received 1 October 2013; Accepted 1 July 2014

Available online 11 November 2014

Abstract. A new numerical method based on locally modified Cartesian meshes is proposed for solving a coupled system of a fluid flow and a porous media flow. The fluid flow is modeled by the Stokes equations while the porous media flow is modeled by Darcy's law. The method is based on a Robin-Robin domain decomposition method with a Cartesian mesh with local modifications near the interface. Some computational examples are presented and discussed.

AMS subject classifications: 65N30, 65N50, 65N55, 76D07, 76S05

Key words: Stokes-Darcy fluid structure interactions, Robin-Robin domain decomposition method, body fitted mesh, locally modified mesh, BJS interface condition.

1. Introduction

The coupled Stokes-Darcy system has recently attracted much attention among researchers. Its applications include flows across interfaces between soil and surface, in areas from oil extraction to bio-medicine. Although individually, the equations for the Stokes-Darcy flows are straightforward and well established, when these two PDE systems are coupled across an interface, there are challenges. The interface conditions between these two systems are the key part. Several conditions have been proposed [2, 8, 14]. In this paper, we consider the well accepted Beavers-Joseph-Saffman (BJS) [8,9,14] interface condition. The existence and uniqueness of weak solutions for the Stokes-Darcy system with BJS interface condition have been proven [10]. Consider

*Corresponding author. *Email addresses:* zwang24@ncsu.edu (Z. Wang), zhilin@ncsu.edu (Z. Li), lubkin@ncsu.edu (S. Lubkin)

the coupled Stokes-Darcy system on a bounded domain $\Omega_p \cup \Omega_f \in \mathbb{R}^d$. The motion of the fluid in Ω_f is modeled by the Stokes equations

$$-\nabla \cdot \mathbf{T}(\mathbf{u}_f, p_f) = \mathbf{f}, \tag{1.1}$$

$$\nabla \cdot \mathbf{u}_f = 0, \tag{1.2}$$

where $\mathbf{u}_f$ is the fluid velocity, p_f is the kinematic pressure, and $\mathbf{f}$ is the body force. $\mathbf{T}(\mathbf{u}_f, p_f) = 2\nu\mathbf{D}(\mathbf{u}_f) - p_f\mathbf{I}$ is the stress tensor and $\mathbf{D}(\mathbf{u}_f) = \frac{1}{2}(\nabla\mathbf{u}_f + \nabla^T\mathbf{u}_f)$ is the strain rate tensor. ∇ and $\nabla\cdot$ represent gradient operator and divergence operator respectively. The parameter $\nu > 0$ in the stress tensor is the kinematic viscosity of the fluid.

In the porous media region Ω_p, the fluid motion is modeled by Darcy's law

$$\mathbf{u}_p = -\mathbf{K}\nabla\phi_p, \tag{1.3}$$

$$\nabla \cdot \mathbf{u}_p = 0, \tag{1.4}$$

where $\mathbf{u}_p$ is the fluid velocity, $\mathbf{K}$ is the hydraulic conductivity tensor, and ϕ_p is the hydraulic head.

On $\Gamma = \Omega_f \cap \Omega_p$, let $\mathbf{n}_f$ denote the unit outward normal vector from Ω_f at Γ and $\mathbf{n}_p$ denote outward normal vector from Ω_p at Γ. $\boldsymbol{\tau}_j$ $(j = 1, \cdots, d-1)$ represents unit tangential vectors on Γ following right hand rule. See Fig. 1 as an example of the domain. Along the interface Γ, if we assume the nondimensional porosity of the Darcy region is 1, we have the mass conservation condition across Γ:

$$\mathbf{u}_f \cdot \mathbf{n}_f = -\mathbf{u}_p \cdot \mathbf{n}_p. \tag{1.5}$$

The second interface condition is the balance of normal stress across Γ:

$$-\boldsymbol{n}_f \cdot (\mathbf{T}(\mathbf{u}_f, p_f) \cdot \mathbf{n}_f) = g\phi_p, \tag{1.6}$$

where g is the acceleration parameter. As the fluid is viscous, a condition for tangential fluid velocity is needed [10]. A simple assumption is free slippage along Γ, $\boldsymbol{\tau}_j \cdot \mathbf{u}_f = 0$.

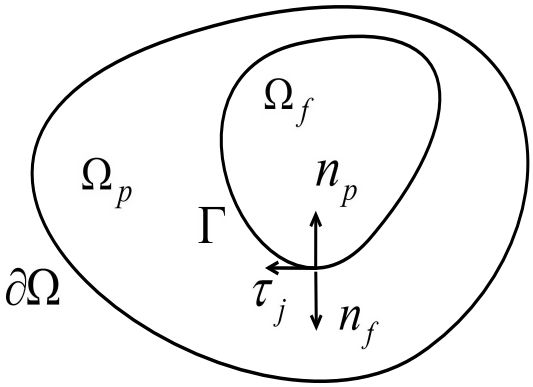

Figure 1: Sketch of a free flow region Ω_f, a porous media region Ω_p, and the interface Γ, the normal direction n_f and tangential direction τ_j, as well as boundary $\partial\Omega$.

But in [2], it is shown that boundary condition agrees with experimental evidence when slip of velocity is proportional to shear stress along Γ. This leads to the full Beavers-Joseph interface condition:

$$\boldsymbol{\tau}_j \cdot (\mathbf{u}_f - \mathbf{u}_p) = \frac{\sqrt{\tilde{k}_j}}{\nu\alpha_1}(-\boldsymbol{\tau}_j \cdot (\mathbf{T}(\mathbf{u}_f, p_f) \cdot \mathbf{n}_f)), \tag{1.7}$$

where $\tilde{k}_j = \boldsymbol{\tau}_j \cdot \nu\mathbf{K} \cdot \boldsymbol{\tau}_j$, and α_1 is some constant. It turns out that the term $\boldsymbol{\tau}_j \cdot \mathbf{u}_p$ is much smaller compared with other terms [2]. In this way we can get the simplified BJS interface condition [9, 14] which is derived from a statistical approach:

$$-\boldsymbol{\tau}_j \cdot (\mathbf{T}(\mathbf{u}_f, p_f) \cdot \mathbf{n}_f) = \alpha\boldsymbol{\tau}_j \cdot \mathbf{u}_f. \tag{1.8}$$

These interface conditions ensure the continuity of velocity and stress in the normal direction across the interface, but the pressure can be discontinuous [6].

The domain decomposition method has been studied by other researchers. The domain decomposition method based on Dirichlet-Neumann type boundary condition is discussed in [5], but it is shown that the method is sensitive to the choice of the kinematic viscosity ν and the hydraulic conductivity tensor $\mathbf{K}$ [6]. The Robin-Robin type domain decomposition method is proposed in [3, 4, 6]. In [6], the Robin-Robin domain decomposition method has been applied to a simplified BJS interface condition. In [4], the parallel Robin-Robin domain decomposition method is carried out for the BJS interface condition and convergence analysis is presented. In [3], the system with BJ interface condition is analyzed, and both parallel and serial domain decomposition methods are constructed. For some complicated domain structures, the mesh generation process might be expensive. In this paper, we consider the locally modified Cartesian mesh method [1, 15]. The main idea of this method is to modify the points at the interface and make them nodal points. Only the points around the interface will be altered and the corresponding mesh will become body fitted. More importantly, the mesh generation cost is negligible as the mesh is transformed from a Cartesian mesh. This method has several applications such as conforming and non-conforming finite element method for elasticity interface problems [7, 11–13]. The objective of this paper is to discuss the feasibility of the Robin-Robin domain decomposition method based on a locally modified mesh and compare the efficiency of unstructured mesh with locally modified mesh.

The paper is organized as follows. In Section 2, we introduce the Robin-Robin domain decomposition method. In Section 3, we discuss the method of locally modified mesh. Finally, in Section 4, some computational examples are presented.

2. Weak formulation and Robin-Robin domain decomposition method

We assume ϕ_p and $\mathbf{u}_f$ are 0 on the boundary $\partial\Omega$ and define the following functional spaces

$$H_f = \{\mathbf{v}_f \in (H^1(\Omega_f))^d \,|\, \mathbf{v}_f = 0 \text{ on } \partial\Omega_f \backslash \Gamma\}, \tag{2.1}$$
$$Q = L^2(\Omega_f), \tag{2.2}$$
$$H_p = \{\psi_p \in H^1(\Omega_p) \,|\, \psi_p = 0 \text{ on } \partial\Omega_p \backslash \Gamma\}. \tag{2.3}$$

The following bilinear forms are defined as

$$a_f(\mathbf{u}_f, \mathbf{v}_f) = 2\nu(\mathbf{D}(\mathbf{u}_f), \mathbf{D}(\mathbf{v}_f)) \quad \text{on } \Omega_f, \tag{2.4}$$
$$a_p(\phi_p, \psi_p) = (\mathbf{K}\nabla\phi_p, \nabla\psi_p) \quad \text{on } \Omega_p, \tag{2.5}$$
$$b_f(\mathbf{v}_f, p_f) = -(\nabla \cdot \mathbf{v}_f, p_f) \quad \text{on } \Omega_f. \tag{2.6}$$

From [3, 4, 6], the weak formulation of the coupled system becomes: finding $(\mathbf{u}_f, p_f)$ $\in H_f \times Q$, $\phi_p \in H_p$ such that

$$\begin{aligned} &a_f(\mathbf{u}_f, \mathbf{v}_f) + b_f(\mathbf{v}_f, p_f) + g a_p(\phi_p, \psi_p) + \langle g\phi_p, \mathbf{v}_f \cdot \mathbf{n}_f\rangle \\ &\quad - \langle g\mathbf{u}_f \cdot \mathbf{n}_f, \psi_p\rangle + \alpha\langle \mathbf{P}_\tau \mathbf{u}_f, \mathbf{P}_\tau \mathbf{v}_f\rangle = (\mathbf{f}, \mathbf{v}_f) \quad \forall \mathbf{v}_f \in H_f, \ \ \psi_p \in H_p, \end{aligned} \tag{2.7}$$
$$b_f(\mathbf{u}_f, q_f) = 0 \quad \forall q_f \in Q, \tag{2.8}$$

where $(\cdot,\cdot)$ denotes L^2 inner product, $\langle\cdot,\cdot\rangle$ denotes L^2 inner product along the interface Γ, and

$$\mathbf{P}_\tau \mathbf{u_f} = \sum_{j=1}^{d-1} (\mathbf{u}_f \cdot \tau_j)\tau_j, \tag{2.9}$$

where $\mathbf{P}_\tau$ denotes projection onto tangential space following right hand rule. $\mathbf{v}_f$, q_f and ψ_p are the corresponding test functions.

Next, we will introduce the Robin-Robin domain decomposition method which is constructed by imposing Robin boundary conditions for the coupled Stokes-Darcy system on the interface. We put tildes above some variables to distinguish them from previous notations.

First, let's consider the Robin boundary condition for the Stokes system

$$\mathbf{n}_f \cdot (\mathbf{T}(\tilde{\mathbf{u}}_f, \tilde{p}_f) \cdot \mathbf{n}_f) + \gamma_f \tilde{\mathbf{u}}_f \cdot \mathbf{n}_f = \eta_f \quad \text{on } \Gamma, \tag{2.10}$$

where $\gamma_f > 0$ is a constant, η_f is a function evaluated on Γ. With the boundary condition on Γ, the weak formulation of the Stokes equations becomes: finding $(\tilde{\mathbf{u}}_f, \tilde{p}_f) \in$ $H_f \times Q$, $\eta_f \in L^2(\Gamma)$ such that

$$\begin{aligned} &a_f(\tilde{\mathbf{u}}_f, \mathbf{v}_f) + b_f(\mathbf{v}_f, \tilde{p}_f) + \gamma_f \langle \tilde{\mathbf{u}}_f \cdot \mathbf{n}_f, \mathbf{v}_f \cdot \mathbf{n}_f\rangle \\ &\quad + \alpha\langle \mathbf{P}_\tau \tilde{\mathbf{u}}_f, \mathbf{P}_\tau \mathbf{v}_f\rangle = (\mathbf{f}, \mathbf{v}_f) + \langle \eta_f, \mathbf{v}_f \cdot \mathbf{n}_f\rangle \quad \forall \mathbf{v}_f \in H_f, \end{aligned} \tag{2.11}$$
$$b_f(\tilde{\mathbf{u}}_f, q_f) = 0 \quad \forall q_f \in Q. \tag{2.12}$$

Next consider the Robin boundary condition for Darcy's law

$$\gamma_p \mathbf{K}\nabla\tilde{\phi}_p \cdot \mathbf{n}_p + g\tilde{\phi}_p = \eta_p \quad \text{on } \Gamma, \tag{2.13}$$

where $\gamma_p > 0$ is a constant and η_p is a function defined similar to η_f unless on Ω_p. The weak formulation of Darcy's law becomes: finding $\tilde{\phi}_p \in H_p$, $\eta_p \in L^2(\Gamma)$ such that

$$\gamma_p a_p(\tilde{\phi}_p, \psi_p) + \langle g\tilde{\phi}_p, \psi_p\rangle = \langle \eta_p, \psi_p\rangle \quad \forall \psi_p \in H_p. \tag{2.14}$$

We combine these weak formulations together. If η_f and η_p are given, there exists a unique solution $(\tilde{\mathbf{u}}_f, \tilde{p}_f) \in H_f \times Q$, $\tilde{\phi}_p \in H_p$ such that

$$\begin{aligned} &a_f(\tilde{\mathbf{u}}_f, \mathbf{v}_f) + b_f(\mathbf{v}_f, \tilde{p}_f) + \gamma_f\langle \tilde{\mathbf{u}}_f \cdot \mathbf{n}_f, \mathbf{v}_f \cdot \mathbf{n}_f\rangle \\ &\quad + \gamma_p a_p(\tilde{\phi}_p, \psi_p) + \langle g\tilde{\phi}_p, \psi_p\rangle + \alpha\langle \mathbf{P}_\tau \tilde{\mathbf{u}}_f, \mathbf{P}_\tau \mathbf{v}_f\rangle \\ &\quad = (\mathbf{f}, \mathbf{v}_f) + \langle \eta_f, \mathbf{v}_f \cdot \mathbf{n}_f\rangle + \langle \eta_p, \psi_p\rangle \quad \forall \mathbf{v}_f \in H_f, \ \ \forall \psi_p \in H_p, \end{aligned} \tag{2.15}$$

$$b_f(\tilde{\mathbf{u}}_f, q_f) = 0 \quad \forall q_f \in Q. \tag{2.16}$$

Finally, to determine appropriate values of functions η_f and η_p, we refer back to Eqs. (2.7), (2.8), which are the weak formulations of the Stokes-Darcy system with BJS interface condition. Eqs. (2.7), (2.8) and (2.15), (2.16) are consistent, i.e., $\mathbf{u}_f = \tilde{\mathbf{u}}_f$, $p_f = \tilde{p}_f$ and $\phi_p = \tilde{\phi}_p$. By subtracting (2.7), (2.8) and (2.15), (2.16), we can get the following equation

$$\begin{aligned} &\gamma_f\langle \mathbf{u}_f \cdot \mathbf{n}_f, \mathbf{v}_f \cdot \mathbf{n}_f\rangle + \gamma_p a_p(\phi_p, \psi_p) + \langle g\phi_p, \psi_p\rangle - g a_p(\phi_p, \psi_p) - \langle g\phi_p, \mathbf{v}_f \cdot \mathbf{n}_f\rangle \\ =&\langle \eta_f, \mathbf{v}_f \cdot \mathbf{n}_f\rangle + \langle \eta_p, \psi_p\rangle \quad \forall \mathbf{v}_f \in H_f, \ \ \forall \psi_p \in H_p. \end{aligned} \tag{2.17}$$

We obtain

$$\langle \eta_f - \gamma_f \mathbf{u}_f \cdot \mathbf{n}_f + g\phi_p, \mathbf{v}_f \cdot \mathbf{n}_f\rangle = 0 \qquad \forall \mathbf{v}_f \in H_f, \tag{2.18}$$

$$\langle \eta_p - g\phi_p, \psi_p\rangle - (\gamma_p - g) a_p(\phi_p, \psi_p) = 0 \quad \forall \psi_p \in H_p. \tag{2.19}$$

Note that η_p and η_f satisfy

$$\eta_f = \gamma_f \mathbf{u}_f \cdot \mathbf{n}_f - g\phi_p, \tag{2.20}$$

$$\eta_p = \gamma_p' \mathbf{u}_f \cdot \mathbf{n}_f + g\phi_p, \tag{2.21}$$

where $\gamma_p' = \gamma_p - g$. We can simply evaluate γ_p' as γ_p without loss of generality and we deduce

$$\eta_f = \gamma_f \mathbf{u}_f \cdot \mathbf{n}_f - g\phi_p, \tag{2.22}$$

$$\eta_p = \gamma_p \mathbf{u}_f \cdot \mathbf{n}_f + g\phi_p. \tag{2.23}$$

Therefore, we have the following algorithm of Robin-Robin domain decomposition method [3,4,6]:

1: For $k = 1, 2, \cdots$, solve the Stokes system (2.11), (2.12) and the Darcy system (2.14) separately, i.e., finding $(\mathbf{u}_f^k, p_f^k) \in H_f \times Q$, $\phi_p^k \in H_p$ such that

$$\begin{aligned} &a_f(\mathbf{u}_f^k, \mathbf{v}_f) + b_f(\mathbf{v}_f, p_f^k) + \gamma_f\langle \mathbf{u}_f^k \cdot \mathbf{n}_f, \mathbf{v}_f \cdot \mathbf{n}_f\rangle + \alpha\langle \mathbf{P}_\tau \mathbf{u}_f^k, \mathbf{P}_\tau \mathbf{v}_f\rangle \\ &\quad = (\mathbf{f}, \mathbf{v}_f) + \langle \eta_f^k, \mathbf{v}_f \cdot \mathbf{n}_f\rangle \quad \forall \mathbf{v}_f \in H_f, \end{aligned} \tag{2.24}$$

$$b_f(\mathbf{u}_f^k, q_f) = 0 \quad \forall q_f \in Q, \tag{2.25}$$

$$\gamma_p a_p(\phi_p^k, \psi_p) + \langle g\phi_p^k, \psi_p\rangle = \langle \eta_p^k, \psi_p\rangle \quad \forall \psi_p \in H_p. \tag{2.26}$$

2: η_f and η_p are updated at each loop as

$$\eta_f^{k+1} = \frac{\gamma_f}{\gamma_p}\eta_p^k + \Big(-1 - \frac{\gamma_f}{\gamma_p}\Big) g\phi_p^k, \tag{2.27}$$

$$\eta_p^{k+1} = -\eta_f^k + (\gamma_f + \gamma_p)\mathbf{u}_f^k \cdot \mathbf{n}_f. \tag{2.28}$$

Initial values of η_p and η_f are chosen arbitrarily. Conditions (2.27), (2.28) are necessary for the convergence of this algorithm. Convergence analysis of this algorithm can be found in [3, 4, 6]. We refer readers to that elegant proof.

3. Local modified Cartesian meshes

In this section, we explain how to get a locally modified Cartesian mesh from a uniform Cartesian mesh. The idea of this method is to perturb the triangulations while keeping the number of nodal points unchanged. The procedure is easy to follow and is shown below:

1: Generate a Cartesian grid. For simplicity, in this paper, we consider a rectangular grid and take the step size the same in both *x* and *y* direction.

2: Locate the intersection of the interface and the grid line. Fig. 2 shows the grid lines and the location of the interface. If the intersection lies between $[x_i - h/2, x_i + h/2] \times [y_i - h/2, y_i + h/2]$, we call the point $[x_i, y_i]$ an irregular point. Otherwise, we call it a regular point.

3: For each irregular point, replace it with an intersection point as a new nodal point. If there is more than one intersection point, the one with smallest distance to the irregular point will be taken. In Fig. 3, the grid point P is an irregular point because the intersection point is within the small dashed rectangle. P1 and P2 are the intersection points. As the distance $d(P, P1) < d(P, P2)$, we take P1 as a new nodal point as demonstrated in Fig. 4.

4: Use the modified nodal points to build triangulations and form a body fitted mesh.

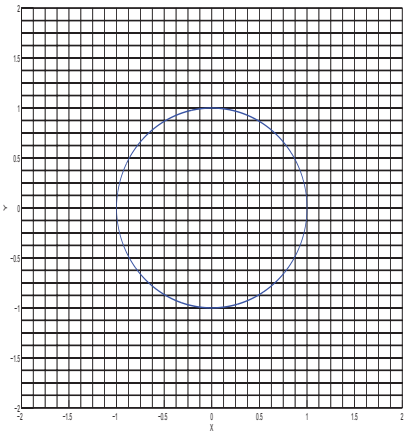

Figure 2: Sketch of the grid lines and the interface without mesh modifications.

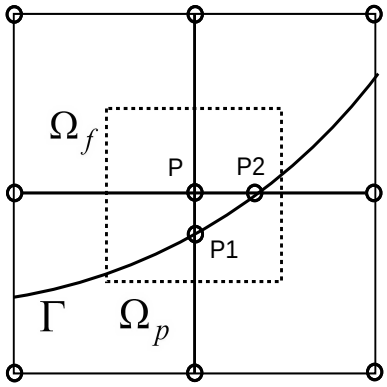

Figure 3: An example of an irregular point and the interface. P1 and P2 are the two points of the intersection between interface Γ and grid lines within the small dashed square $[x_i - h/2, x_i + h/2] \times [y_i - h/2, y_i + h/2]$ of irregular point P. The area on the left of Γ is Ω_f, on the right is Ω_p.

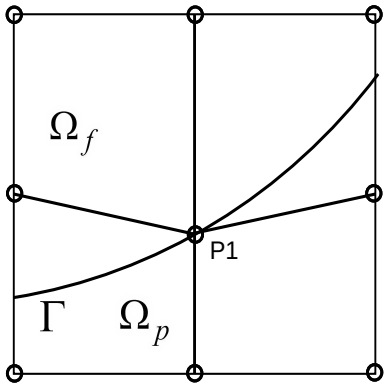

Figure 4: An example of a modified point. Point P is replaced by point P1 and the total number of nodal points remains unchanged.

It has been proven in [1] that if the interface $\Gamma \in \mathcal{C}^2$, the accuracy of the approximation of the interface Γ is $\mathcal{O}(h^2)$. Fig. 5 is an example of the locally modified mesh in which the interface is a circle. We can see that only the points around the circular interface are altered and the total number of nodal points remain unchanged.

4. Numerical examples

In this section we present two numerical examples of the coupled nondimensional Stokes-Darcy system with a circular interface. Consider a case in $\mathbb{R}^2$. Let Ω_f be a unit circle centered at $(0, 0)$ with radius 1. Ω_p is the square of $[-2, 2] \times [-2, 2]$ outside the unit circle. See Fig. 6 as an illustration. The unstructured mesh is shown in Fig. 7 while the locally modified mesh is constructed and is shown is Fig. 5. For simplicity, choose

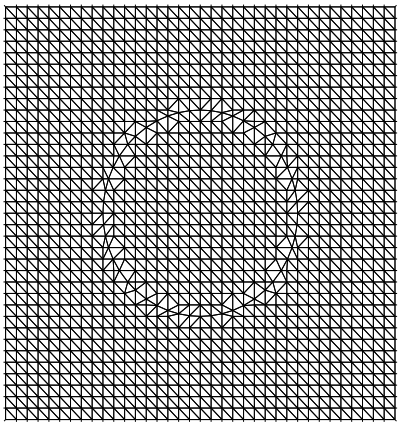

Figure 5: A locally modified mesh example where step number $n = 32$ (32 points on each side of the square) in both x and y direction. The triangulations are built using the modified nodal points.

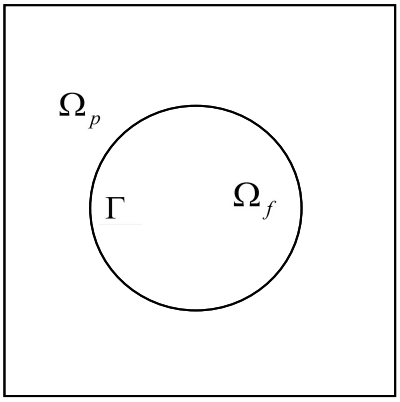

Figure 6: A computational example with circular interface Γ.

$\nu = 1$, $g = 1$, $\mathbf{K} = \mathbf{I}$, $\alpha = 1$. An analytic solution of (2.7), (2.8) is given by

$$u_1 = y(x^2 + y^2 - 3), \quad u_2 = -x(x^2 + y^2 - 3), \quad p_f = x^2 + y^2,$$
$$f_1 = -8y + 2x, \quad f_2 = 8x + 2y, \quad \phi_p = 1. \tag{4.1}$$

The boundary conditions on $\partial\Omega$ are determined accordingly. These analytic solutions satisfy the Stokes-Darcy system with circular interface as well as the BJS interface condition. For the finite element approximation, the Taylor-Hood element pair is used for the Stokes equations which is quadratic in velocity and linear in pressure. A linear finite element space is used for Darcy's law. The dimension of finite element space of the coupled Stokes-Darcy system is consistent on the interface. As discussed in [3,4,6], we choose $\gamma_f = 3\gamma_p$ for convergence of the algorithm. In Table 1, the H^1 norm error of velocity $\mathbf{u}_f$, and the L^2 norm error of $\mathbf{u}_f$, p_f and ϕ_p are reported. Table 2 shows

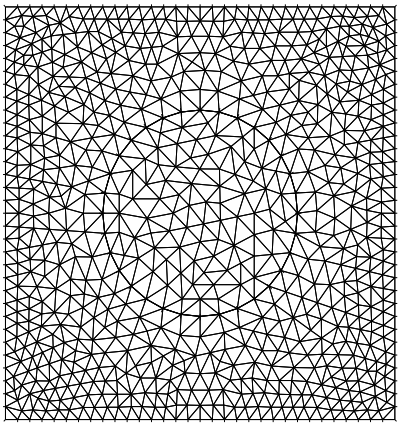

Figure 7: An unstructured mesh example where step number $n = 32$ in both x and y direction.

Table 1: An error report of unstructured mesh method with various step numbers.

Step number n	L^2 error of $\mathbf{u}_f$	H^1 error of $\mathbf{u}_f$	L^2 error of p_f	L^2 error of ϕ_p
16	7.83e-2	2.02e-1	5.34e-2	1.61e-2
20	5.11e-2	1.45e-1	4.31e-2	1.26e-2
32	2.02e-2	8.29e-2	2.09e-2	8.02e-3
40	1.29e-2	6.80e-2	1.31e-2	6.20e-3
64	5.01e-3	5.02e-2	4.11e-3	3.84e-3
80	3.25e-3	4.34e-2	3.08e-3	3.11e-3
128	1.28e-3	3.53e-2	2.41e-3	2.02e-3

Table 2: An error report of locally modified mesh method with various step numbers.

Step number n	L^2 error of $\mathbf{u}_f$	H^1 error of $\mathbf{u}_f$	L^2 error of p_f	L^2 error of ϕ_p
16	3.74e-2	1.14e-1	4.21e-2	1.07e-2
20	2.73e-2	9.71e-2	2.71e-2	1.06e-2
32	1.18e-2	6.36e-2	1.20e-2	6.36e-3
40	6.90e-3	5.40e-2	7.61e-3	5.26e-3
64	2.50e-3	4.11e-2	3.40e-3	2.94e-3
80	1.75e-3	3.74e-2	2.91e-3	2.57e-3
128	6.70e-4	2.90e-2	2.01e-3	1.71e-3

the error report based on locally modified mesh method. We compare the two methods (Table 3) for a locally modified mesh of 2048 elements and an unstructured mesh of 2100 elements (260 Stokes, 1840 Darcy). The two methods have comparable error. Therefore the method of locally modified mesh is not only free of mesh generation, but also provides comparable accuracy. Table 4 compares convergence order as the slope

Table 3: A comparison of the two methods based on a similar number of triangulations.

Method	Elements	L^2 error of $\mathbf{u}_f$	H^1 error of $\mathbf{u}_f$	L^2 error of p_f	L^2 error of ϕ_p
unstructured mesh	2100	1.43e-2	7.11e-2	5.74e-3	6.70e-3
locally modified mesh	2048	1.18e-2	6.36e-2	1.20e-3	6.36e-3

Table 4: A comparison of the convergence order of unstructured mesh and locally modified mesh.

		Unstructured mesh		Locally modified mesh	
Quantity	Norm	Slope	R^2	Slope	R^2
$\mathbf{u}_f$	L^2	1.98	0.99	1.97	0.99
$\mathbf{u}_f$	H^1	0.83	0.96	0.67	0.98
p_f	L^2	1.67	0.97	1.44	0.96
ϕ_p	L^2	1.01	0.99	0.94	0.99

of the log-log plots of error against grid fineness n. As usual, the H^1 norm error of $\mathbf{u}_f$ is approximately one order less than the L^2 norm error of $\mathbf{u}_f$. Fig. 8 shows the velocity computed using the locally modified mesh for the example (4.1).

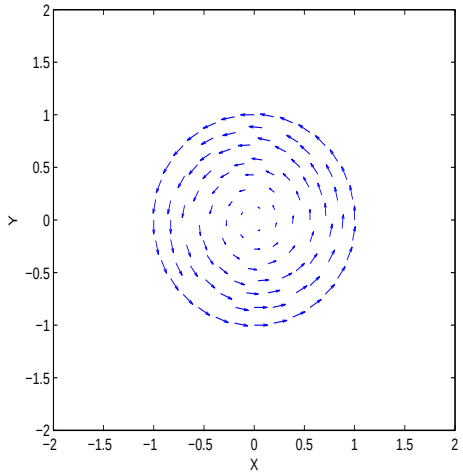

Figure 8: A plot of the fluid velocity in the coupled Stokes-Darcy system for the example (4.1). As Φ_p=1, the fluid velocity in porous media region Ω_p, in this case, outside the unit circle, is 0.

We now provide a more realistic example. In Fig. 9, a simulation of the Stokes-Darcy interaction is shown by assuming the fluid velocity on the boundary is $(0, -1)$. The parameter values ν, g, $\mathbf{K}$ and α are set the same as in the previous example. The overall flow is downwards with faster flow in the Stokes region due to the coupling at the interface, corresponding to flow in a void in a porous medium such as soil.

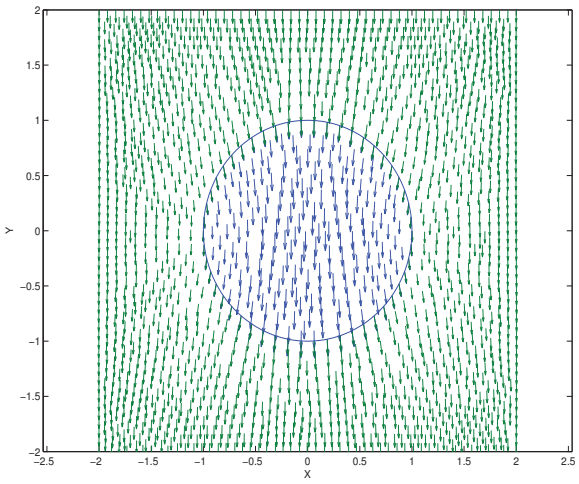

Figure 9: A simulation of the Stokes-Darcy interaction with parameters $\nu = 1$, $g = 1$, $\mathbf{K} = \mathbf{I}$ and $\alpha = 1$. The fluid of Darcy's law moves downwards and interacts with the fluid of Stokes equations.

5. Conclusions

In this paper we discussed the Stokes-Darcy system. A set of analytic solutions is constructed for the coupled system with a circular interface. The methods of locally modified mesh and unstructured mesh are compared and the Robin-Robin domain decomposition with locally modified mesh provides comparable accuracy and convergence order to that with an unstructured mesh. For the Stokes-Darcy system with complex domain structures, the Robin-Robin domain decomposition method based on a locally modified mesh might be more efficient then a potentially costly unstructured mesh. For future research, the full Navier-Stokes equations coupled with Darcy's law shall be an interesting topic.

Acknowledgments The authors are supported in part by the US-NIH grant R01GM096195. The second author is also partially supported by the US AFSOR grant FA9550-09-1-0520, and the NCSU Innovation Seed grant.

References

[1] C. Börgers. A triangulation algorithm for fast elliptic solvers based on domain imbedding. *SIAM J. Numer. Anal.*, 27:1187–1196, 1990.

[2] G. Beavers and D. Joseph. Boundary conditions at a naturally permeable wall. *J. Fluid Mech.*, 30:197–207, 1967.

[3] Y. Cao, M. Gunzburger, X. He, and X. Wang. Robin-Robin domain decomposition methods for the steady-state Stokes-Darcy system with the Beavers-Joseph interface condition. *Numer. Math.*, 117:601–629, 2011.

[4] W. Chen, M. Gunzburger, F. Hua, and X. Wang. A parallel Robin-Robin domain decomposition method for the Stokes-Darcy system. *SIAM J. Numer. Anal.*, 49(3):1064–1084, 2011.
[5] M. Discacciati and A. Quarteroni. Convergence analysis of a subdomain iterative method for the finite element approximation of the coupling of Stokes and Darcy equations. *Comput. Vis. Sci.*, 6(2-3):93–103, 2004.
[6] M. Discacciati, A. Quarteroni, and A. Valli. Robin-Robin domain decomposition methods for the Stokes-Darcy coupling. *SIAM J. Numer. Anal.*, 45(3):1246–1268, 2007.
[7] Y. Gong, B. Li, and Z. Li. Immersed-interface finite-element methods for elliptic interface problems with non-homogeneous jump conditions. *SIAM J. Numer. Anal.*, 46:472–495, 2008.
[8] W. Jäger and A. Mikelić. On the interface boundary condition of Beavers, Joseph, and Saffman. *SIAM J. Appl. Math.*, 60(4):1111–1127, 2000.
[9] I. Jones. Low Reynolds number flow past a porous spherical shell. *Proc. Camb. Phil. Soc.*, 73:231–238, 1973.
[10] W.J. Layton, F. Schieweck, and I. Yotov. Coupling fluid flow with porous media flow. *SIAM J. Numer. Anal.*, 40(6):2195–2218, 2002.
[11] Z. Li, T. Lin, and X. Wu. New Cartesian grid methods for interface problem using finite element formulation. *Numer. Math.*, 96:61–98, 2003.
[12] Z. Li and P. Song. An adaptive mesh refinement strategy for immersed boundary/interface methods. *Commun Comput Phys.*, 12(2):515–527, 2012.
[13] Z. Li and P. Song. Adaptive mesh refinement techniques for the immersed interface method applied to flow problems. *Computers and Structures*, 122:249–258, 2013.
[14] P. Saffman. On the boundary condition at the interface of a porous medium. *Stud. Appl. Math.*, 1:77–84, 1971.
[15] H. Xie, K. Ito, Z. Li, and J. Toivanen. A finite element method for interface problems with locally modified triangulation. *Contemporary Mathematics*, 466:179–190, 2008.